(4-Hydroxyphenyl)pyruvate Dioxygenase from *Streptomyces avermitilis*: The Basis for Ordered Substrate Addition†

Kayunta Johnson-Winters, Vincent M. Purpero, Michael Kavana, Tamara Nelson, and Graham R. Moran,*

Department of Chemistry, University of Wisconsin—Milwaukee, 3210 N. Cramer Street, Milwaukee, Wisconsin 53211-3029

Received July 23, 2002; Revised Manuscript Received December 18, 2002

ABSTRACT: (4-Hydroxyphenyl)pyruvate dioxygenase (HPPD) catalyzes the second step in the pathway for the catabolism of tyrosine, the conversion of (4-hydroxyphenyl)pyruvate (HPP) to homogentisate (HG). This reaction involves decarboxylation, substituent migration, and aromatic oxygenation. HPPD is a member of the α-keto acid dependent oxygenases that require Fe(II) and an α-keto acid substrate to oxygenate an organic molecule. We have examined the binding of ligands to HPPD from *Streptomyces avermitilis*. Our data show that HPP binds to the apoenzyme and that the apo-HPPD·HPP complex does not bind Fe(II) to generate active holoenzyme. The binding of HPP, phenylpyruvate (PPA), and pyruvate to the holoenzyme produces a weak ligand charge-transfer band at ∼500 nm that is indicative of bidentate binding of the 1-carboxylate and 2-keto pyruvate oxygen atoms to the active site metal ion. For HPPD from this organism the 4-hydroxyl group of (4-hydroxyphenyl)pyruvate is a requirement for catalysis; no turnover is observed in the presence of phenylpyruvate. The rate constant for the dissociation of Fe(II) from the holoenzyme is 0.0006 s^{-1} and indicates that this phenomenon is not significantly relevant in steady-state turnover. The addition of HPP and molecular oxygen to the holoenzyme is formally random. The basis of the ordered bi bi steady-state kinetic mechanism previously observed by Rundgren (Rundgren, M. (1977) *J. Biol. Chem. 252*, 5094−9) is the 3600-fold increase in oxygen reactivity when holo-HPPD is in complex with HPP. This complex reacts with molecular oxygen with a second-order rate constant of 1.4×10^5 M^{-1} s^{-1} inducing the formation of an intermediate that decays at the catalytically relevant rate of 7.8 s^{-1}.

(4-Hydroxyphenyl)pyruvate dioxygenase (EC 1.13.11.27, HPPD)[1] catalyzes the extraordinary conversion of (4-hydroxyphenyl)pyruvate (HPP) to homogentisate (HG), a reaction involving decarboxylation, substituent migration, and aromatic oxygenation (Scheme 1). This reaction is ubiquitous in aerobic metabolism and is the second step in the pathway for the catabolism of tyrosine. HPPD is a member of the α-keto acid dependent oxygenases that require Fe(II) and an α-keto acid (typically α-ketoglutarate) to oxygenate an organic substrate. The most studied examples of this family are prolyl hydroxylase, clavaminate synthase, and cephalosporin C synthase (*1*, *2*). Within this large family of enzymes, HPPD is the exception as it catalyzes the incorporation of both atoms of molecular oxygen into a single substrate; the requisite α-keto acid is provided from the pyruvate substituent of HPP.

Continued interest in HPPD has arisen from a number of specific high-affinity inhibitors of the enzyme (*3*−*7*). In man, one of these inhibitors is used to treat type 1 tyrosinemia, an otherwise lethal inherited defect in the final step of tyrosine catabolism (*8*, *9*). In plants, inhibition of HPPD has been found to have significant herbicidal activity, preventing the production of plastoquinone (*10*−*14*).

Scheme 1

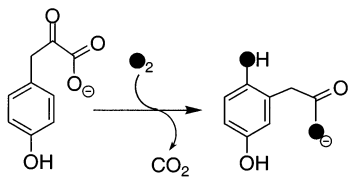

The crystal structures of ferrous iron dependent oxygenases have revealed a common mononuclear iron binding motif in which the metal ion is coordinated to two histidines and one acid residue. Water molecules occupy the remaining ligand sites of either square pyramidal or octahedral coordination spheres (*15*). Due to facile oxidation of coordinated Fe(II) in an oxygenated atmosphere, the majority of structural data available are from the oxidized and inactive ferric form of these enzymes. The only examples structurally solved under anaerobic conditions in their active ferrous form are the α-keto acid dependent enzymes, deacetoxycephalosporin synthase, taurine dioxygenase (TauD), clavaminate synthase, and anthocyanidin synthase (*16*−*19*). Each of these structures were solved in the presence of one or more of their organic

† This research was supported by the National Institutes of Health (Grant DK59551-01A1) to G.R.M. and in part by the American Chemical Society Petroleum Research Fund (Grant 36169-G4) to G.R.M.

* To whom correspondence should be addressed. Ph: (414) 229 5031. Fax: (414) 229 5530. E-mail: moran@uwm.edu.

[1] Abbreviations: HEPES, *N*-(2-hydroxyethyl)piperizine-*N*′-ethanesulfonic acid; HPPD, (4-hydroxyphenyl)pyruvate dioxygenase; HPP, (4-hydroxyphenyl)pyruvate; PPA, phenylpyruvate; HG, (2,5-dihydroxyphenyl)acetate; SDS, sodium docecyl sulfate.

10.1021/bi026499m CCC: $25.00
Published on Web 01/30/2003

substrates and thus have provided significant geometric insight into the activation of these enzymes toward a reaction with molecular oxygen. In these structures, α-ketoglutarate is bound bidentate via one of the carboxylate and the α-keto oxygen atoms. Recently, the crystal structure of oxidized HPPD from *Pseudomonas fluorescens* was solved (*20*). The active site ligands to the iron are the same as those observed in other mononuclear Fe(II)-dependent enzymes (*21*).

Steady-state kinetic experiments indicate that HPPD has an ordered bi bi mechanism in which HPP is the first substrate to bind and carbon dioxide is the first product to dissociate (*22*). This suggests that HPP is an activating effector for the reaction of HPPD with molecular oxygen, inducing the formation of the first oxygenated intermediate. This apparent substrate-induced activation of the enzyme is consistent with what has been proposed for other Fe(II)-dependent oxygenases (*1, 23*−*27*).

A number of the fundamental aspects of the chemistry carried out by HPPD are established. It has been shown that only oxygen atoms from molecular oxygen are incorporated into HG. These form the 2-hydroxyl and one of the carboxylate oxygens (*28*) (Scheme 1). It has also been established that a proton ortho to the pyruvate substituent of HPP is lost during the migration of the decarboxylated, now aceto, side chain to the adjacent carbon (*29*). This movement of the aceto side chain is perhaps the clearest example in nature of what is known as the NIH shift. This shift is a well documented, though poorly understood substituent migration phenomenon observed with P-450, pterin-dependent and other aromatic oxygenases (*30*−*38*). In these enzymes, the mechanism of migration has remained in dispute for more than 30 years and substituents larger than tritium typically migrate in only a minor fraction of total catalysis (*35, 39*−*42*). The 100% efficient migration of the large aceto substituent in HPPD is therefore unique.

Despite the medical and agricultural significance of HPPD and the intriguing chemistry of the reaction catalyzed, there is a dearth of evidence that pertains to the chemical mechanism. Plausible chemical mechanisms have been offered but with little or no direct evidence for the existence of discrete catalytic steps (*29, 43, 44*). Recent pre-steady-state analyses of the α-keto acid dependent dioxygenase, TauD, have demonstrated that spectrophotometrically detectable intermediates can occur in these enzymes (*45*). Here, we present for HPPD from *Streptomyces avermitilis* the first direct evidence for the order of substrate addition in turnover, the nature of substrate acquisition particularly with respect to molecular oxygen, and evidence of intermediate accumulation.

EXPERIMENTAL PROCEDURES

Materials. HPP, HG, PPA, pyruvate, MES, HEPES buffers, and iron(II) ammonium sulfate were purchased from ACROS. (2-Hydroxyphenyl)acetic acid was purchased from Avacado Research Chemicals Ltd. α-Ketoglutarate was from ICN Biochemicals. Ammonium sulfate was from Fisher Scientific. Dithiothreitol and sodium acetate were purchased from Sigma. Q-Sepharose and Sephacryl S-200 were obtained from Bio-Rad. Pelleted Luria-Bertani broth (LB) was purchased from BIO101. Isopropyl β-thiogalactopyranoside (IPTG) was from United States Biochemicals. Streptomycin sulfate, ampicillin, and electrophoretic grade agarose were obtained from ICN Biomedicals, Inc. Ferene S (3-(2-pyridyl)-5,6-bis(2-[5-furylsulfonic acid])-1,2,4-triazine) was purchased from Sigma. Plasmid pET17b was obtained from Novagen. Chemically competent TOP10 and BL21 (DE3) *Escherichia coli* were purchased from Invitrogen. Restriction and DNA modification enzymes were purchased from New England Biolabs. Plasmids were purified using the Qiagen midi prep plasmid preparation kit and protocol.

Subcloning. The 1.2 Kb gene for HPPD from *S. avermitilis* was from the plasmid pCD661 (*46*). This gene was subcloned into pET17b (Novagen) by restriction with *Nde* I and *BamH* I. The ligation mixture was used to transform chemically competent TOP10 *E. coli* cells and spread onto LB agar, 100 μg/mL ampicillin. Individual colonies were used to inoculate 5 mL of LB broth, 100 μg/mL ampicillin. The plasmids from each of these cultures were then purified using the Qiagen miniprep plasmid purification protocol and screened using *Nde* I and *BamH* I restriction for the gene insert. The resulting 4489 bp plasmid, pSAHPPD, was then sequenced in the region of the HPPD gene and used to transform chemically competent BL21 (DE3) *E. coli* cells.

Protein Expression and Purification of Apo-HPPD. Aliquots from frozen cell stocks were plated (240 μL/L of culture) on LB agar, 100 μg/mL ampicillin. After incubation for 9−12 h at 37 °C, the cells from two plates were resuspended in ∼10 mL of LB broth and used to inoculate 1 L of LB broth, 100 μg/mL ampicillin. The culture was grown with vigorous shaking (225 rpm) at 37 °C until the cell density had reached an OD_{600} of 1.0. At this time, IPTG was added to a final concentration of 0.2 mM and incubation was continued for 2.5 h. The cells were harvested by centrifugation at 4665*g* for 30 min and used immediately for protein purification.

Unless otherwise stated, all subsequent purification procedures were undertaken at 4 °C. Cells were resuspended using 20 mL of 20 mM HEPES, 1 mM EDTA, pH 7.0, per L of culture and lysed with sonication (2 × 5 min at 45 W) using a Branson sonicator fitted with a blunt tungsten tip. The temperature of the solution was monitored to ensure that it did not exceed 10 °C. The lysed cells were then centrifuged at 11 200*g* for 30 min, and the pellet was discarded. Streptomycin sulfate in water was then added to the supernatant to a final concentration of 1.5% w/v. The mixture was stirred for 10 min and centrifuged at 11 200*g* for 20 min. The supernatant was brought to 45% $(NH_4)_2SO_4$ saturation over a period of 20 min and centrifuged at 7800*g* for 10 min. The resulting supernatant was then brought to 65% $(NH_4)_2SO_4$ saturation over a period of 20 min and centrifuged at 7800*g* for 10 min. The pellet obtained from this step was redissolved in 20 mM HEPES, 1 mM EDTA, pH 7.0, using 50 mL/L of initial culture and loaded directly onto a Q-Sepharose column (22 cm^3 L^{-1} of culture) equilibrated in the above buffer. The protein was eluted with a linear 350 mL gradient to 400 mM NaCl in the same buffer. The fractions containing HPPD activity were combined (70−100 mL) and then concentrated to ∼3 mL using a Biomax 10 kDa cutoff centrifugal filter and applied to an S-200 size exclusion column (245 cm^3) at a flow rate of 1 mL/min. The enzyme was eluted with 20 mM HEPES, pH 7.0. The fractions containing HPPD were pooled and stored at −80 °C.

Calibrated Size Exclusion Chromatography. An S-200 size exclusion column (220 cm^3) was calibrated by loading a 2 mL mixture of ribonuclease A (13.7 kDa, 2 mg/mL), chymotrypsinogen (25 kDa, 2 mg/mL), ovalbumin (43 kDa, 2 mg/mL), albumin (67 kDa 2 mg/mL) and blue dextran (1 mg/mL) in 20 mM HEPES, pH 7.0. The mixture was loaded and eluted at a flow rate of 1 mL/min in the same buffer. Individual proteins were detected as they eluted using a Bio-Rad model EM-1 absorbance detector coupled to a Bio-Rad model 1327 chart recorder. A calibration curve was made by plotting the elution volume against the logarithm of each components molecular weight. Purified HPPD (2 mL, 4 mg/mL) was applied at a flow rate of 1 mL/min and eluted under the same conditions.

Enzyme Assays and Steady-State Observations. Routine enzyme assays were performed using a model DW1 Hansetech Oxygraph oxygen electrode. The 1 mL reaction mixture contained 10 μM ferrous ammonium sulfate, 1 mM dithiothreitol, and HPPD (typically 50−750 nM) in 20 mM HEPES buffer, pH 7.0. After initial observation of the nonenzymatic rate of oxygen consumption due to Fenton chemistry, the enzymatic reaction was initiated by the addition of HPP. Dissolved oxygen concentration was controlled prior to the addition of the enzyme by sparging the assay mixture for 10 min with blended ratios of nitrogen and oxygen gases supplied from a MAXblend Maxtec gas mixer with an in-line oxygen sensor coupled to Timeter low volume flow tube. Plots of activity versus substrate concentration were fit using Kaleidagraph software (Synergy) to either the Michaelis−Menten equation (eq 1) or, in the case of substrate inhibition, to eq 2 that has an additional term to account for the inhibition and gives an estimate of K_i.

$$v = \frac{V_{max}[S]}{K_m + [S]} \quad (1)$$

$$v = \frac{V_{max}[S]}{K_m + [S] + ([S]^2/K_i)} \quad (2)$$

Steady-state kinetic constants were determined for HPPD by simultaneously varying the concentrations of molecular oxygen (37−254 μM) and HPP (6−818 μM). The 1 mL assay mixture contained 5 μM ferrous ammonium sulfate, 1 mM dithiothrietol, and 200 nM HPPD in 20 mM HEPES, pH 7.0. For consistency, assays were initiated with equal volumes of serially diluted HPP stocks after the reaction mixture had been sparged for 10 min in a defined oxygen partial pressure. The data obtained were compiled into a single set which was fit to determine steady-state kinetic constants using Nonlin (Rubelko Software) to eq 3 which describes an ordered bi bi steady-state system.

$$v = \frac{(V_{max}[HPP][O_2])}{(K_{i\,HPP}K_{O_2}) + (K_{HPP}[O_2]) + (K_{O_2}[HPP]) + ([HPP][O_2])} \quad (3)$$

Extinction Coefficients. At equilibrium, under conditions of neutral pH, HPP has an absorbance maximum at 276 nm. The extinction coefficient at this wavelength was measured by a combination of spectrophotometric and electrochemical methods based on the known stoichiometry of the HPPD reaction. A Hansetech oxygen electrode was used to measure the concentration of oxygen consumed when HPPD (2 μM final) was added to an assay mixture as described above, in which the concentration of HPP was limiting and its absorbency was known. Using this method the equilibrium extinction coefficient of HPP was found to be 2,800 M^{-1} cm^{-1}. The 280 nm extinction coefficient of HPPD was calculated for the unfolded peptide by the method of Pace (*47*) (40 465 M^{-1} cm^{-1}). The absorbance spectrum of the folded apoenzyme was compared to that of the SDS (1% w/v) denatured protein to determine the 280 nm extinction coefficient for the folded state (41 200 M^{-1} cm^{-1}).

Iron Determination. Dissolved iron concentrations were measured using the Fe(II) specific chelator Ferene S. The complex of Ferene S and Fe(II) has an absorbance maximum at 592 nm (ϵ_{592} = 35 500 M^{-1} cm^{-1}) (*48*). To ensure all iron was in the ferrous form, ascorbate was added to a final concentration of 1 mM prior to the addition of Ferene S. To determine iron-to-subunit ratios for pure enzyme samples, SDS to a final concentration of 1% w/v was added prior to the addition of ascorbate. In each case, Ferene S was then added to a final concentration of 400 μM.

Fe(II) Dissociation. The rate of release of Fe(II) from the HPPD·Fe(II) complex was observed with a stopped-flow spectrophotometer under anaerobic conditions by mixing limiting concentrations (10−20 μM) of the complex with excess (0.5−1 mM) of the Fe(II) chelator, Ferene S, in 20 mM HEPES, pH 7.0, at 4 °C. As Fe(II) was released from the HPPD·Fe(II) complex, the formation of the stable Fe(II)·[Ferene S]$_2$ complex was observed at 592 nm and fit to a single exponential to determine the rate constant for Fe(II) dissociation.

Binding of α*-Keto Acids to HPPD*. The α-keto acids, HPP, PPA, pyruvate, and α-ketoglutarate, were examined as active site ligands for HPPD. A 4 mL solution of apo-HPPD (400 μM) in 20 mM HEPES buffer was made anaerobic by 36 cycles of vacuum and argon in a tonometer at 4 °C. Once anaerobic, ferrous ammonium sulfate was added from a side arm to a concentration of 395 μM. The tonometer was then mounted onto a Hitech model-SF61-DX2 stopped-flow spectrophotometer. α-Keto acid ligand solutions were prepared anaerobically by sparging each with argon gas for 10 min prior to mounting onto the stopped-flow instrument. Each α-keto acid was titrated to the holoenzyme at 4 °C by mixing initially with a concentration that matched the holo-HPPD concentration and subsequently with increased concentrations. The spectrum of the enzyme (300−700 nm) in the presence of each ligand concentration was taken, and the concentration of the ligand was increased until no further change in the spectrum between 400 and 700 nm was observed. For each ligand, the spectral contribution of the free α-keto acid was subtracted and the pure ligand complex spectrum was determined.

Substrate Specificity and Product Analyses for α*-Keto Acids*. PPA, α-ketoglutarate, and pyruvate were examined as substrates for HPPD using an oxygen electrode. A series of 2 mL reaction mixtures contained 15 μM ferrous ammonium sulfate, 1 mM dithiothreitol, varied HPPD (1−5 μM), and varied α-keto acid concentration (0.1−2.0 mM) in 20 mM HEPES buffer, pH 7.0. After initial observation of the nonenzymatic rate of oxygen consumption due to

Fenton chemistry, the enzymatic reaction was initiated by the addition of the α-keto acid and monitored for 10 min. The rate of oxygen consumption ($t = 0-180$ s) after to the addition of α-keto acid was compared to rate of oxygen consumption prior to its addition.

(2-Hydroxyphenyl)acetic acid is the expected product of coupled turnover of HPPD with PPA (*49*). Each of the reaction mixtures described above for PPA was analyzed for the presence of this product by HPLC. Each assay was ultrafiltred through a Biomax 0.5 mL 10 kDa cutoff filter to remove HPPD. This solution was then diluted 10-fold in 20 mM HEPES, and 20 μL of this solution was applied to a Waters Xterra reverse phase (C18) analytical column (4.6 × 50 mm). The components of the reaction were separated isocratically at 1 mL/min in 20 mM sodium acetate pH 5.5 using a Waters 600E multisolvent delivery system coupled to a Waters 2487 dual λ absorbance detector for detection at 280 nm. Data were acquired and analyzed using Peak Simple software (SRI). These data were compared to a standard curve for (2-hydroxyphenyl)acetic acid (6 pmol−1.57 μmol) prepared for the authentic compound under the same conditions.

Dissociation Constants for the HPPD−Ligand Complexes. The dissociation constant for HPP binding to apo-HPPD was measured using a Jasco model J-715 circular dichroism spectrophotometer. Apo-HPPD (63 μM) was titrated with HPP to saturation which was observed as a small ellipticity decrease between 238 and 244 nm (Δ(molar) ellipticity ∼ 8000). From these values the unbound substrate concentration ($[\text{ligand}]_f$) could be deduced for each concentration and plotted against the fractional saturation (f) to determine the dissociation constant (K_d) according to eq 4.

$$f = \frac{[\text{ligand}]_f}{K_d + [\text{ligand}]_f} \quad (4)$$

The dissociation constants for HPP and PPA binding to the HPPD·Fe(II) complex were measured using a adaptation of the methods of Ryle et al. (*45*). A 4 mL solution of apo-HPPD was made anaerobic by 36 cycles of vacuum and argon in a tonometer at 4 °C (260 and 400 μM for respective HPP and PPA titrations). Once anaerobic, ferrous ammonium sulfate was added from a side arm to a final concentration 10 μM less than that of HPPD. To provide accurate, temperature-controlled mixing under anaerobic conditions, the tonometer was then mounted onto a stopped-flow instrument and mixed with a range of anaerobic solutions of ligand (HPP or PPA) prepared by sparging for 10 min with argon. The binding of either HPP or PPA to the active site of the enzyme could be observed as a broad, weak absorbance signal with a maximum at ∼500 nm. The fractional saturation of the enzyme sample (f) was determined from the fractional change of this absorbance feature with each ligand addition. From these values the free ligand concentration ($[\text{ligand}]_f$) could be deduced and plotted to determine the dissociation constant according to eq 4.

Stopped-Flow Measurements. Pre-steady-state analysis of HPPD was undertaken using a Hi-Tech model SF61-DX2 stopped-flow spectrophotometer. The measured dead time of this instrument was 1.6 ms. The reaction of the HPPD·Fe(II) complex with molecular oxygen was observable as an increase due to Fe(III) formation at 320 nm. Anaerobic ferrous holoenzyme (20 μM final concentration; comprised of 50 μM HPPD and 40 μM Fe(II) initial concentration) was prepared as above and mixed with a range of oxygen concentrations that gave pseudo-first-order conditions (0.24−1.3 μM final concentration) at 4 °C. The observed rate constants were then plotted against oxygen concentration and fit to a straight line according to eq 5.

$$k_{obs} = k[O_2] \quad (5)$$

To observe the reaction of the HPPD·Fe(II)·HPP complex with molecular oxygen, a 1.024 mM solution of the HPPD·HPP complex (1.024 mM HPPD, 1.5 mM HPP) in 20 mM HEPES buffer, pH 7.0, was made anaerobic in a tonometer by 36 cycles of vacuum and argon. Once anaerobic, ferrous ammonium sulfate in 10 mM HCl was added to a final concentration of 1.0 mM from a calibrated threaded barrel syringe attached to the tonometer. The tonometer was then mounted onto the stopped-flow instrument. A solution of oxygenated buffer was prepared under atmospheric pressure by equilibrating a blend of nitrogen and oxygen to give 1.0 mM oxygen at 4 °C. This solution was then mixed with the anaerobic HPPD·Fe(II)·HPP complex at 4 °C, and the reaction was monitored at 490 nm. The resulting absorbance traces were simulated using Chemical Kinetics Simulator software (IBM) and compared using Kaliedagraph software (Synergy) to provide estimates of extinction coefficients and rate constants. The inverse of the molecular oxygen concentration was plotted against time for the determination of the rate constant for the reduction of molecular oxygen by the HPPD·Fe(II)·HPP complex according to eq 6, where $[O_2]_0$ is the concentration at time zero (*50*).

$$1/[O_2] = 1/[O_2]_0 + kt \quad (6)$$

RESULTS

Subcloning, Expression, and Purification. The sequence of the subcloned HPPD gene from *S. avermitilis* revealed three additional bases at position 120 in the gene that are not part of the published sequence for the HPPD gene from this organism (shown italicized, 5′ 109 GCG CAC TAC T*AC T*CC ACC GCC 3′) (*46*). These bases span two codons and code for an additional tyrosine corresponding to position 41 in the protein. It is suggested that these bases reveal an error in the published sequence since their inclusion produces improved homology to the amino acid sequences of HPPD from other organisms.

The T7 polymerase based pET expression system of Studier (*51*) was used to express HPPD. Restriction subcloning using *Nde* I and *BamH* I into plasmid pET17b placed the HPPD gene 7 bases from the ribosome binding site. On the basis of SDS-PAGE densitometry for cell lysates harvested 2 h after induction at 37 °C, HPPD was expressed as 30−35% of the total cell protein.

HPPD was purified in three steps over 36 h; these were $(NH_4)_2SO_4$ fractionation, a Q-sepharose chromatography, and an S-200 size exclusion chromatography (Table 1). The enzyme was eluted from Q-Sepharose at a NaCl concentration of 180 mM. Calibrated S-200 size exclusion chromatography revealed that the elution volume of purified HPPD correlated with a molecular weight of 51 kDa most consistent

Table 1: Summary of the Purification of HPPD from *S. avermitilis* Heterologously Expressed from 1 L of BL21 DE3 *E. coli*

procedure	protein (mg)	tot. activity (U)[a]	specific activity (U/mg)[a]
sonicate	190	532	2.8
streptomycin supernatant	151	453	3.0
45% AS[b] supernatant	122	366	3.0
65% AS pellet	65	391	6.0
65% AS supernatant	9	4	0.4
Q-Sepharose column eluate	44	370	8.4
S-200 column eluate	38	404	10.6

[a] U refers to enzymatic activity in μmol/min. [b] AS refers to ammonium sulfate.

with the enzyme being predominantly monomeric (calculated monomer molecular weight, 41.7 kDa).

When purified in the absence of a chelator, the enzyme contained 0.4 Fe atoms/monomer and had an amethyst color due to a weak absorbance feature at 608 nm ($\epsilon_{608\ nm} = 3062$ M^{-1} cm^{-1} based on the iron concentration). The yield and specific activity of the purified enzyme was enhanced by the inclusion of EDTA to 1 mM during the sonication, streptomycin sulfate, ammonium sulfate precipitation, and anion exchange chromatography purification steps. The omission of EDTA from the size exclusion chromatographic step permitted preparation of the apoenzyme devoid of the chelator. When EDTA was included from purification buffers, the resulting purified enzyme contained no detectable iron (<0.05 atom/monomer). A typical yield from 1 L of cells was 30−50 mg of purified enzyme with a specific activity of 10 μmol HG produced/(min mg) (7 s^{-1}) in the presence of ferrous ammonium sulfate. The enzyme in this form was stable at room temperature and could be stored at −80 °C indefinitely without loss of activity. Relatively low concentrations of HPPD (<100 μM) were stable at room temperature for at least 16 h, while solutions of higher concentration slowly accumulated turbidity due to enzyme denaturation and as such were routinely studied at 4 °C.

Rate of Dissociation of Fe(II) from HPPD. The release of Fe(II) from the HPPD·Fe(II) complex was observable in the presence of the Fe(II) specific chelator Ferene S. The formation of the stable, strongly absorbing Fe(II)·(Ferene $S)_2$ complex was used as an indicator for the release of Fe(II) from the holoenzyme. When anaerobic HPPD·Fe(II) was mixed with excess Ferene S under anaerobic conditions, the rate of formation of the 592 nm spectral feature was 0.0006 s^{-1} and was independent of HPPD and Ferene S concentrations. In such an experiment, it is a requirement that the rate of association of Ferene S with Fe(II) be more rapid than the rate of release of Fe(II) from the HPPD·Fe(II) complex. As such, the rate of formation of Ferene S−Fe(II) complex was measured separately under anaerobic conditions in 20 mM HEPES, pH 7.0, at 4 °C. The rate of formation of the Fe(II)·(Ferene $S)_2$ absorbance feature was second order in Ferene S and had an association rate constant of 3.16×10^5 M^{-2} s^{-1}. This indicated that, at the concentrations used, the Ferene S−Fe(II) association rate is at least 8000-fold more rapid and thus sufficient to permit observation of the rate of Fe(II) release from the holoenzyme complex.

Substrate Specificity. HPP, PPA, pyruvate, and α-ketoglutarate were examined as substrates for HPPD. Of the aromatic substrates, only HPP was oxygenated, producing exclusively (2,5-dihydroxyphenyl)acetate (homogentistate). No evidence of oxygen uptake could be observed in the presence of α-ketoglutarate, pyruvate, or PPA. No (2-hydroxyphenyl)acetic acid could be detected by HPLC when high concentrations of HPPD were incubated with a range of PPA concentrations under conditions of atmospheric oxygen. Prior to chromatographic separation each reaction was ultrafiltered to remove HPPD; the efficiency of elution of (2-hydroxyphenyl)acetic acid from the filter membrane was 94.6%. Under the conditions chosen, the retention times of the keto and enol forms of PPA were 2.20 and 4.46 min, respectively, while (2-hydroxyphenyl)acetic acid eluted at 3.36 min when either injected as the pure dissolved compound or when added to the enzymatic reaction mixtures. The lower limit of detection under these conditions was 6 pmol of (2-hydroxyphenyl)acetic acid indicating that a turnover rate as low as 0.000 01 s^{-1} would have been detected. No additional components were observed in samples containing HPPD compared to control samples to which the enzyme was not added.

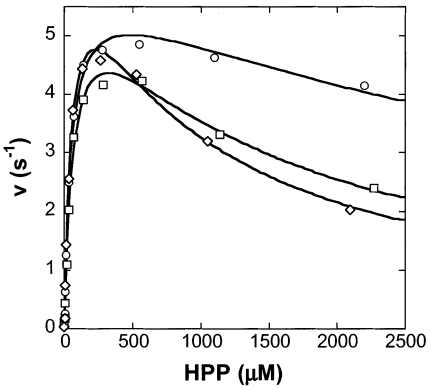

FIGURE 1: Steady-state kinetic analyses for HPP. Assays were performed using a model DW1 Hansetech Oxygraph oxygen electrode. The 2 mL reaction mixture contained 254 μM molecular oxygen, 10 μM ferrous ammonium sulfate, 1 mM dithiothreitol, and HPPD (500 nM) in 20 mM HEPES buffer, pH 7.0, 25 °C. The enzymatic reaction was initiated either by the addition of HPPD (◇), Fe(II) (□), or HPP (○) in the presence of all other reaction components.

Of the α-keto acids listed above, only HPP, PPA, and pyruvate could be observed to form active site complexes with holo-HPPD that produce a charge-transfer transition (Figure 2) (*45*, *52*−*54*). The absence of a charge-transfer band in the presence of α-ketoglutarate may be a result weak binding to the HPPD·Fe(II)·α-ketoglutarate complex. However, verification of a saturating condition for this ligand was not possible as concentrations greater than 2 mM induced significant denaturation of the holoenzyme. Together, these data suggest that, for this form of the enzyme, the presence of the 4-hydroxyl of HPP is a requirement for catalysis but not a requirement for bidentate association of an α-keto acid with the active site metal ion.

Steady-State Kinetic Analyses for HPPD. Steady-state kinetic parameters were determined for HPP and molecular oxygen (Table 2). With HPP, significant substrate inhibition was seen at elevated substrate concentrations when assays were initiated with either HPPD or Fe(II) ($K_i = 0.82 \pm 0.12$ and 1.32 ± 0.22 mM, respectively, Figure 1). Less inhibition was observed when HPP was used to initiate assays ($K_i = 4.52 \pm 0.99$ mM). This strongly suggests that the apoenzyme

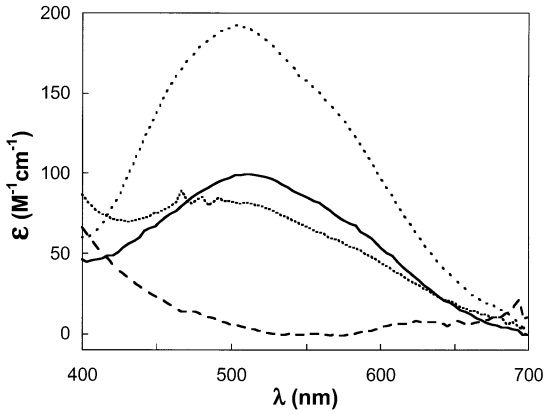

FIGURE 2: Difference spectra of HPPD·Fe(II) in the presence of α-keto acids. An amount of 195 μM HPPD was mixed anaerobically with (—) 800 μM (4-hydroxyphenyl)pyruvate, (· · ·) 2.5 mM phenylpyruvate, (···) 5 mM pyruvate, and (— — —) 2 mM α-ketoglutarate in 20 mM HEPES, pH 7.0, at 4 °C. For each spectrum the contribution of the unbound ligand was subtracted.

Table 2: Steady-State Kinetic Parameters for HPPD from *S. avermitilis*

param	value[a]	param	value[a]
V_{max} (s^{-1})	6.8 ± 0.6	V/K_{HPP} (mM^{-1} s^{-1})	254 ± 70
K_{HPP} (μM)	27 ± 6	V/K_{O_2} (mM^{-1} s^{-1})	98 ± 21
K_{O_2} (μM)	69 ± 19		

[a] Measured at 25 °C, in the presence of 200 nM HPPD, 5 μM ferrous ammonium sulfate, 1 mM DTT, and 20 mM HEPES buffer, pH 7.0.

is able to bind HPP and the resulting complex (apo-HPPD·HPP) is slow to dissociate and does not permit the binding of ferrous iron (Scheme 2). Steady-state kinetic parameters were determined by simultaneously varying the concentrations of molecular oxygen and HPP in a single kinetic experiment. From these data, the extrapolated turnover number at 25 °C based on the fit to eq 3 is 7 s^{-1}. The K_m for molecular oxygen was 70 μM, indicating that the enzyme is approximately 80% saturated in oxygen under atmospheric conditions.

Dissociation Constants for HPPD Complexes. To examine the binding of HPP to apo-HPPD, the apoenzyme was titrated with HPP and the perturbation of the CD spectrum was monitored. In the absence of Fe(II), a saturating spectral phenomenon is observed as HPP is titrated to apo-HPPD. The fit to eq 4 indicated a relatively low-affinity HPPD·HPP complex whose dissociation constant was 179 ± 46 μM at 25 °C.

The binding of HPP and PPA to the holoenzyme could be observed anaerobically in titration as a broad, weak increase in absorbance at ~500 nm (Figure 2). To ensure a measurable concentration of free ligands existed at equilibrium throughout the titration, the concentration of enzyme

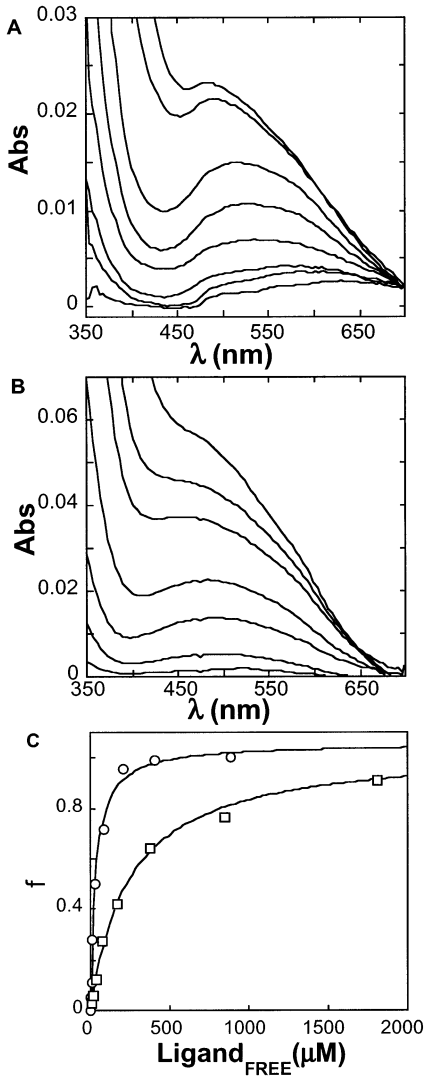

FIGURE 3: Titration of holo-HPPD with HPP and PPA under anaerobic conditions: (A) difference spectra observed in the titration of 124 μM holo-HPPD with HPP (7.5−1030 μM); (B) difference spectra observed in the titration of 200 μM holo-HPPD with PPA (15−4000 μM); (C) fractional saturation of HPPD versus free HPP (○) and free PPA (□) concentration fit to eq 4. To avoid free ligand spectral contributions, absorbance changes at 520 nm were used for analysis.

was systematically reduced in a series of such titrations until significant curvature was observed in the plot of $Abs_{520\ nm}$ vs HPP_{total}. When the fractional saturation from such an experiment was calculated and plotted against free HPP concentration the dissociation constant was determined from the fit of the data to eq 4 (Figure 3). In contrast to the apo-HPPD·HPP complex, the dissociation constant for the holo-HPPD·HPP complex is 6-fold lower at 32.4 ± 3.3 μM, indicating a role for Fe(II) in substrate binding to the

Scheme 2

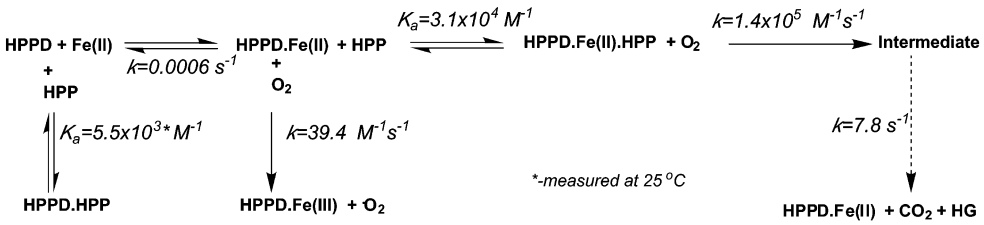

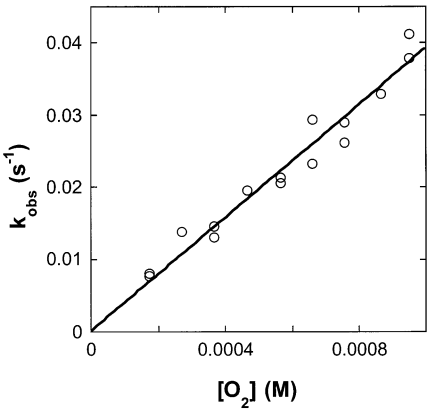

FIGURE 4: Oxidation of the HPPD·Fe(II) complex by molecular oxygen as observed at 320 nm. The anaerobic HPPD·Fe(II) complex (25 μM HPPD, 20 μM Fe(II) final) was mixed with various oxygen concentrations in a stopped-flow spectrophotometer at 4 °C.

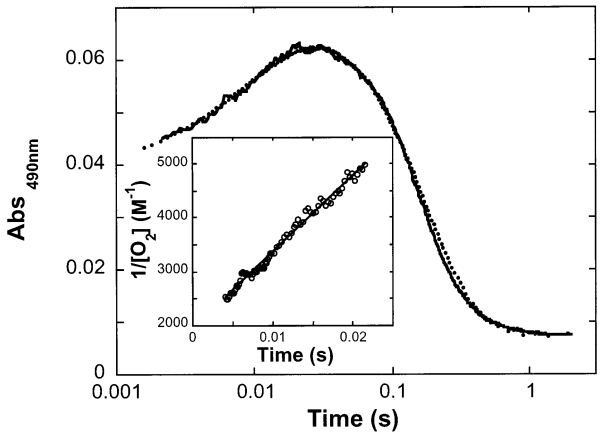

FIGURE 5: Reaction of the HPPD·Fe(II)·HPP complex (512 μM final) with molecular oxygen (512 μM final) at pH 7.0 and 4 °C as observed at 490 nm. The simulation of these data to Scheme 3 with rate constants defined as $k_1 = 1.4 \times 10^5$ M^{-1} s^{-1} ($\Delta\epsilon = 90$ M^{-1} cm^{-1}) and $k_2 = 7.8$ s^{-1} ($\Delta\epsilon = 152$ M^{-1} cm^{-1}) is shown as a dotted line overlaying the absorbance trace. Inset: determination of the second-order rate constant for the reaction of the HPPD·Fe(II)·HPP complex with molecular oxygen as calculated from the initial increase in absorbance fit to eq 6.

holoenzyme. The dissociation constant for the holo-HPPD·PPA complex was 243 ± 20 μM, 8-fold higher than the native substrate under the same conditions. This indicates a relatively small energetic contribution ($\Delta\Delta G = -4.6$ kJ/mol) of the HPP 4-hydroxyl to the formation of the HPPD·Fe(II)·HPP complex.

Oxygen Reduction by HPPD. Both the free holoenzyme and the holoenzyme in complex with HPP react with molecular oxygen. When anaerobic enzyme was mixed with molecular oxygen, the oxidation of the free holoenzyme (20 μM final) was observed at 320 nm. At this wavelength, the HPPD·Fe(III) complex has significant absorbance ($\epsilon_{320\ nm} \sim$ 2200 M^{-1} cm^{-1}). Approximately 90% of the observed amplitude could be fit to a single exponential. A plot of the observed rate constant for this process against molecular oxygen concentration (0.2−1 mM) is linear and intercepts the origin. The second-order rate constant for addition of oxygen to the enzyme calculated from the slope was 39.2 ± 0.8 M^{-1} s^{-1} (Figure 4).

The HPPD·Fe(II)·HPP complex was observed to react with molecular oxygen using a stopped-flow spectrophotometer at wavelengths between 245 and 750 nm. While it was clear that this phenomenon has an oxygen dependence, accurate assignment of the rate constants (particularly at low oxygen concentration) was hindered by the low extinction coefficient changes for this process. To measure the magnitude of the rate constant for the reduction of molecular oxygen by the HPPD·Fe(II)·HPP complex, matched concentrations of both reactants (HPPD·Fe(II)·HPP and O_2) were used (Figure 5). In such an experiment the integrated rate expression is not exponential (eq 6).

A plot of the inverse of the reactant concentration against time yields a straight line for second-order processes, the intercept of which should equal the inverse of the concentration of either reactant at time zero (inset Figure 5). The rate constant, derived from the slope, was $1.43 \times 10^5 \pm 1.6 \times 10^3$ M^{-1} s^{-1}, based on an extinction coefficient change of 90 M^{-1} cm^{-1}, 3600-fold faster than the reduction of molecular oxygen in the absence of HPP. The absorbance change at this wavelength is biphasic, indicating the reaction of the enzyme−substrate complex with molecular oxygen coincides with the accumulation of an intermediate. Due to the apparent large rate constant differential between the first and the second phase of this process, absorbance data beyond 80 ms could be fit to a single exponential where the observed intermediate decayed at the catalytically relevant rate of 7.8 s^{-1}. The entire reaction trace could be simulated to two kinetic steps in which a bimolecular reaction is followed by a first-order process where k_1 was defined 1.45×10^5 M^{-1} s^{-1} and k_2 was 7.8 s^{-1}, consistent with the values determined from our analysis of the data (Scheme 3). On the basis of the measured rate constants, the maximal fractional accumulation of the intermediate is 60%. The magnitude of the net extinction coefficient change for both phases of the trace is 75 M^{-1} cm^{-1}, consistent with the disappearance of the long-wavelength charge transfer observed in the holoenzyme−substrate complex resulting from the proposed bidentate binding of HPP to the active site metal ion (Figure 2). This biphasic process was not observed in control experiments conducted under the same conditions in the absence of either the enzyme or the substrate.

Scheme 3

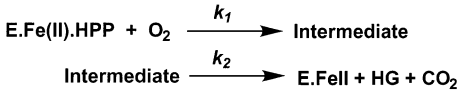

DISCUSSION

HPPD is a member of the α-keto acid dependent oxygenases, all of which have highly similar coordination environments for the mononuclear Fe(II) ion and could be predicted to have similar strategies for the reduction of molecular oxygen. HPPD is the exception within this family as it has two rather than three substrates and incorporates both atoms of molecular oxygen into a single organic molecule (Scheme 1). For these oxygenases a consensus is emerging as to the order of binding of substrates. Thorough steady-state analyses now exist for prolyl hydroxylase (*55*, *56*), thymine hydroxylase (*57*), lysyl hydroxylase (*58*), deacetoxyvindoline hydroxylase (*59*), and HPPD (*22*). In all cases partially or fully ordered steady-state mechanisms are observed, in which typically the α-keto acid is the first substrate to bind and CO_2 is the first product to dissociate. Since HPPD has only

two substrates, the order is HPP (α-keto) followed by molecular oxygen. With such a high degree of accord for the steady-state mechanisms of such enzymes, there is little impetus to independently determine by such methods the substrate binding mechanism for HPPD from *S. avermitilis*. Instead, more explicit evidence for both the order of addition of substrates to HPPD and the equilibrium constants and/or rate constants for the formation and decay of such complexes was the primary objective of experiments described here.

HPPD from *S. avermitilis* expresses to high levels in *E. coli* and can be purified in three steps to a specific activity of 10 μmol of HG produced/(min mg) (7 s^{-1}). This rate of turnover compares favorably with that observed in preparations of HPPD from carrot (1.91 s^{-1}) (*60*), from *Pseudomonas fluorescens* (0.67 s^{-1}) (*20*), human (0.71 s^{-1}) (*22*), and pig (8.3 s^{-1}) (*61*). Calibrated size exclusion chromatography of the purified enzyme suggests that this form of HPPD is predominately monomeric in solution. This is consistent with what has been observed by such methods for HPPD from other bacteria and eukaryotes. However, for HPPD from these other organisms, analytical ultracentrifugation methods reveal weak associations for the formation of tetramers and dimers for bacteria and eukaryotes respectively (*62*−*64*). Thus, the observation of a monomer here is useful in the preparation of the pure enzyme but remains to be verified as the true oligomeric state in solution.

Observation of HPPD in the steady state using varied HPP concentrations reveals significant substrate inhibition when assays are initiated with either Fe(II) or apo-HPPD, and little inhibition is observed when HPP is used. This implies that HPP and Fe(II) bind randomly to the apoenzyme and the apo-HPPD·HPP complex is unable to bind Fe(II) (Scheme 2). The dissociation constant of the apo-HPPD·HPP complex (∼180 μM) is consistent with this assertion and would suggest that when assays are initiated with either apo-HPPD or Fe(II), measured initial rates would be determined for enzyme that is partially inhibited by the HPP concentration used.

Possibly the most intriguing observation of this investigation is that PPA is not a substrate for HPPD from *S. avermitilis*. Though PPA binds only 8-fold less tightly to the holoenzyme than does HPP, HPLC product analysis and oxygen uptake experiments clearly show that PPA does not significantly activate HPPD for a reaction with molecular oxygen and that it is not a substrate. It is therefore clear that the 4-hydroxyl group of HPP is a requirement for substrate recognition yet has only a modest contribution (−4.6 kJ/mol) to the HPP binding energy. This differs from mammalian HPPD isoforms that are reported to use HPP, PPA, and α-ketoisocaproate as substrates (*49*, *65*).

The absorbance feature at ∼500 nm observed when holo-HPPD is titrated anaerobically with HPP, PPA, or pyruvate is similar in shape and intensity to those observed with the mechanistically related enzymes TauD and (2,4-dichlorophenoxy)acetate dioxygenase (TfdA) (*45*, *52*) (Figure 2). The crystal structure of TauD in complex with α-ketoglutarate shows that this substrate is bound bidentate to the active site iron through coordination to the 1-carboxylate and 2-keto oxygen atoms (*17*). This feature has recently been probed using resonance Raman and is believed to be associated with transition from the α-keto/carboxylate HOMO to its π^* LUMO (*54*). For TauD and TfdA, this absorbance is present when α-ketoglutarate binds the holoenzyme. The transitions shift slightly to shorter wavelengths and the transitions become more resolved when the second organic substrate is added to this complex. The consensus for these enzymes is that when both substrates are bound, reactivity toward molecular oxygen increases though this has not been formally quantified. For these enzymes square pyramidal iron geometry is observed in the presence of both organic substrates, leaving the octahedral ligand site open (*66*). On this basis, it is reasonable to speculate that in the presence of its native α-keto acid substrate, HPP, the active site iron of holo-HPPD is largely five coordinate and poised to react with molecular oxygen.

To probe the oxygen reactivity of holo-HPPD in the presence and absence of HPP, the free holoenzyme and the substrate in complex with the holenzyme were reacted with molecular oxygen. The 3600-fold acceleration in the rate of oxygen reduction in the presence of HPP definitively establishes an activating effector role for the α-keto substrate in this enzyme. Furthermore, this is the basis of the steady-state observation of ordered addition in productive catalysis (Scheme 3). The fact that the reciprocal of the oxygen concentration during the first phase of the reaction is linear with time throughout a concentration change of 500 μM suggests that this reaction is reliant solely on collision and there is no formal requirement for oxygen to reversibly bind to the HPPD·Fe(II)·HPP complex for catalysis to occur. Alternatively, the dissociation constant for molecular oxygen from the HPPD·Fe(II)·HPP·O_2 complex may be relatively large (≥500 μM). Of considerable interest is the accumulation and decay of an intermediate when the HPPD·Fe(II)·HPP complex reacts with molecular oxygen. The first-order oxygen dependence of the formation of this intermediate indicates that this is the first oxygenated species to accumulate in turnover. Furthermore, the accurate simulation of these data to a minimal kinetic scheme establishes that the time frame of these processes is relevant to turnover and within reach of freeze quench experiments for characterization of the intermediate using other spectroscopies. We are currently undertaking experiments under pseudo-first-order conditions to define the spectrum of this and other observable intermediates in the hope that the intermediate can ultimately be trapped and further characterized.

The above data reveal random combination of the apoenzyme with Fe(II) and HPP and random combination of the holoenzyme with HPP and molecular oxygen. However, classification of the steady-state substrate binding mechanism as ordered remains accurate as a consequence of the respective slow release of Fe(II) from the holoenzyme, low affinity of the apoenzyme for HPP, and slow rate of oxidation of the holoenzyme in the absence of HPP.

These data are the first to define actual complex affinities for HPPD from any source and are the basis for the order of addition of substrates to the enzyme in normal turnover. Knowledge of the magnitude of these affinities will serve as the foundation for further biophysical investigation of this medically and agriculturally important enzyme.

ACKNOWLEDGMENT

We are grateful to Claudio Denoya (Pfizer) for supplying plasmid pCD661 containing the HPPD gene from *S. avermitilis*. We also thank Robert Ponton (University of

Wisconsin−Milwaukee) for the design and tireless modification of specialized glassware to conduct anaerobic experiments.

REFERENCES

1. Solomon, E. I., Brunold, T. C., Davis, M. I., Kemsley, J. N., Lee, S. K., Lehnert, N., Neese, F., Skulan, A. J., Yang, Y. S., and Zhou, J. (2000) *Chem. Rev. 100*, 235−350.
2. Que, L. J., and Ho, R. Y. N. (1996) *Chem. Rev. 96*, 2607−2524.
3. Lin, S. W., Lin, Y. L., Lin, T. C., and Yang, D. Y. (2000) *Bioorg. Med. Chem. Lett. 10*, 1297−8.
4. Romagni, J. G., Meazza, G., Nanayakkara, N. P., and Dayan, F. E. (2000) *FEBS Lett. 480*, 301−5.
5. Ellis, M. K., Whitfield, A. C., Gowans, L. A., Auton, T. R., Provan, W. M., Lock, E. A., and Smith, L. L. (1995) *Toxicol. Appl. Pharmacol. 133*, 12−9.
6. Ellis, M. K., Whitfield, A. C., Gowans, L. A., Auton, T. R., Provan, W. M., Lock, E. A., Lee, D. L., and Smith, L. L. (1996) *Chem. Res. Toxicol. 9*, 24−27.
7. Schulz, A., Ort, O., Beyer, P., and Kleinig, H. (1993) *FEBS Lett. 318*, 162−6.
8. Lindblad, B., Lindstedt, S., and Steen, G. (1977) *Proc. Natl. Acad. Sci. U.S.A. 74*, 4641−5.
9. Lindstedt, S., Holme, E., Lock, E. A., Hjalmarson, O., and Strandvik, B. (1992) *Lancet 340*, 813−7.
10. Mitchell, G., Bartlett, D. W., Fraser, T. E., Hawkes, T. R., Holt, D. C., Townson, J. K., and Wichert, R. A. (2001) *Pestic. Manage. Sci. 57*, 120−8.
11. Pallett, K. E., Cramp, S. M., Little, J. P., Veerasekaran, P., Crudace, A. J., and Slater, A. E. (2001) *Pestic. Manage. Sci. 57*, 133−42.
12. Lin, Y. L., Wu, C. S., Lin, S. W., and Yang, D. Y. (2000) *Bioorg. Med. Chem. Lett. 10*, 843−5.
13. Dyson, J. S., Beulke, S., Brown, C. D., and Lane, M. C. (2002) *J. Environ. Qual. 31*, 613−8.
14. Wu, C. S., Huang, J. L., Sun, Y. S., and Yang, D. Y. (2002) *J. Med. Chem. 45*, 2222−8.
15. Lange, S. J., and Que, L. (1998) *Curr. Opin. Chem. Biol. 2*, 159−172.
16. Valegard, K., van Scheltinga, A. C., Lloyd, M. D., Hara, T., Ramaswamy, S., Perrakis, A., Thompson, A., Lee, H. J., Baldwin, J. E., Schofield, C. J., Hajdu, J., and Andersson, I. (1998) *Nature 394*, 805−9.
17. Elkins, J. M., Ryle, M. J., Clifton, I. J., Dunning Hotopp, J. C., Lloyd, J. S., Burzlaff, N. I., Baldwin, J. E., Hausinger, R. P., and Roach, P. L. (2002) *Biochemistry 41*, 5185−92.
18. Zhang, Z., Ren, J., Harlos, K., McKinnon, C. H., Clifton, I. J., and Schofield, C. J. (2002) *FEBS Lett. 517*, 7−12.
19. Wilmouth, R. C., Turnbull, J. J., Welford, R. W., Clifton, I. J., Prescott, A. G., and Schofield, C. J. (2002) *Structure (London) 10*, 93−103.
20. Serre, L., Sailland, A., Sy, D., Boudec, P., Rolland, A., Pebay-Peyroula, E., and Cohen-Addad, C. (1999) *Struct. Fold Des. 7*, 977−88.
21. Hegg, E. L., and Que, L., Jr. (1997) *Eur. J. Biochem. 250*, 625−9.
22. Rundgren, M. (1977) *J. Biol. Chem. 252*, 5094−9.
23. Arciero, D. M., Orville, A. M., and Lipscomb, J. D. (1985) *J. Biol. Chem. 260*, 14035−44.
24. Shu, L., Chiou, Y. M., Orville, A. M., Miller, M. A., Lipscomb, J. D., and Que, L., Jr. (1995) *Biochemistry 34*, 6649−59.
25. Brown, C. A., Pavlosky, M. A., Westre, T. E., Zhang, Y., Hedman, B., Hodgson, K. O., and Solomon, E. I. (1995) *J. Am. Chem. Soc. 117*, 715−732.
26. Roach, P. L., Clifton, I. J., Hensgens, C. M., Shibata, N., Schofield, C. J., Hajdu, J., and Baldwin, J. E. (1997) *Nature 387*, 827−30.
27. Harpel, M. R., and Lipscomb, J. D. (1990) *J. Biol. Chem. 265*, 22187−96.
28. Lindblad, B., Lindstedt, G., and Lindstedt, S. (1970) *J. Am. Chem. Soc. 92*, 7446−7449.
29. Rundgren, M. (1982) *Biochim. Biophys. Acta 704*, 59−65.
30. Sono, M., Roach, M. P., Coulter, E. D., and Dawson, J. H. (1996) *Chem. Rev. 96*, 2841−2888.
31. Fitzpatrick, P. (1998) in *Comprehensive Biological Catalysis* (Sinnot, M., Ed.) Vol. III, pp 181−194, Academic Press, New York.
32. Daly, J. W., Jerina, D. M., and Witkop, B. (1972) *Experientia 28*, 1129−1264.
33. Bowman, W. R., Gretton, W. R., and Kirby, G. W. (1980) *J. Chem. Soc. PerkinTrans. 2*, 218.
34. Guroff, G., Daly, J. W., Jerina, D. M., Renson, J., Witkop, B., and Udenfriend, S. (1967) *Science 157*, 1524−1530.
35. Jerina, D. M., Daly, J. W., and Witkop, B. (1968) *J. Am. Chem. Soc. 90*, 6523−6525.
36. Jerina, D. M., Daly, J. W., and Witkop, B. (1971) *Biochemistry 10*, 366−372.
37. Kurata, T., Watanabe, Y., Katoh, M., and Sawaki, Y. (1988) *J. Am. Chem. Soc. 110*, 7472−7478.
38. Leinberger, R., Hull, W. E., Simon, H., and Retey, J. (1981) *Eur. J. Biochem. 117*, 311−8.
39. Kasperek, G. J., Bruice, T. C., Yagi, H., and Jerina, D. M. (1972) *J. Chem. Soc., Chem. Commun*. 784−785.
40. Fitzpatrick, P. F. (1994) *J. Am. Chem. Soc. 116*, 1133−1134.
41. Hillas, P. J., and Fitzpatrick, P. F. (1996) *Biochemistry 35*, 6969−6975.
42. Moran, G. R., Derecskei-Kovacs, A., Hillas, P. J., and Fitzpatrick, P. F. (2000) *J. Am. Chem. Soc. 122*, 4535−4541.
43. Pascal, R. A., Jr., Oliver, M. A., and Chen, Y. C. (1985) *Biochemistry 24*, 3158−65.
44. Hamilton, G. A. (1971) in *Progress in Biorganic Chemistry* (Kaiser, E. T., and Kezdy, F. J., Eds.) Vol. 1, pp 83−157, John Wiley and Sons, Inc., New York.
45. Ryle, M. J., Padmakumar, R., and Hausinger, R. P. (1999) *Biochemistry 38*, 15278−15286.
46. Denoya, C. D., Skinner, D. D., and Morgenstern, M. R. (1994) *J. Bacteriol. 176*, 5312−9.
47. Pace, N. C., Vajdos, F., Fee, L., Grimsley, G., and Gray, T. (1995) *Protein Sci. 4*, 2411−2423.
48. Higgins, T. (1981) *Clin. Chem. 27*, 1619−20.
49. Denum, J., Lindstedt, S., and Rundgren, M. (1982) in *Oxidases and Related Redox Systems* (King, T. E., Mason, H. S., and Morrison, M., Eds.) pp 519−542, Pergamon Press, Albany, NY.
50. Tinoco, I., Sauer, K., and Wang, J. C. (1995) *Physical Chemistry: Principles and Applications in Biological Sciences*, 3rd ed., Prentice Hall, Upper Saddle River, NJ.
51. Studier, F. W., and Moffatt, B. A. (1986) *J. Mol. Biol. 189*, 113−130.
52. Hegg, E. L., Whiting, A. K., Saari, R. E., McCracken, J., Hausinger, R. P., and Que, L., Jr. (1999) *Biochemistry 38*, 16714−26.
53. Hogan, D. A., Smith, S. R., Saari, E. A., McCracken, J., and Hausinger, R. P. (2000) *J. Biol. Chem. 275*, 12400−9.
54. Ho, R. Y., Mehn, M. P., Hegg, E. L., Liu, A., Ryle, M. J., Hausinger, R. P., and Que, L., Jr. (2001) *J. Am. Chem. Soc. 123*, 5022−9.
55. Tuderman, L., Myllyla, R., and Kivirikko, K. I. (1977) *Eur. J. Biochem. 80*, 341−8.
56. Myllyla, R., Tuderman, L., and Kivirikko, K. I. (1977) *Eur. J. Biochem. 80*, 349−57.
57. Holme, E. (1975) *Biochemistry 14*, 4999−5003.
58. Puistola, U., Turpeenniemi-Hujanen, T. M., Myllyla, R., and Kivirikko, K. I. (1980) *Biochim. Biophys. Acta 611*, 51−60.
59. De Carolis, E., and De Luca, V. (1993) *J. Biol. Chem. 268*, 5504−11.
60. Garcia, I., Job, D., and Matringe, M. (2000) *Biochemistry 39*, 7501−7.
61. Roche, P. A., Moorehead, T. J., and Hamilton, G. A. (1982) *Arch. Biochem. Biophys. 216*, 62−73.
62. Wada, G. H., Fellman, J. H., Fujita, T. S., and Roth, E. S. (1975) *J. Biol. Chem. 250*, 6720−6.
63. Lindblad, B., Lindstedt, G., Lindstedt, S., and Rundgren, M. (1977) *J. Biol. Chem. 252*, 5073−84.
64. Buckthal, D. J., Roche, P. A., Moorehead, T. J., Forbes, B. J., and Hamilton, G. A. (1987) *Methods Enzymol. 142*, 132−8.
65. Crouch, N. P., Lee, M. H., Iturriagagoitia-Bueno, T., and MacKinnon, C. H. (2000) *Methods Enzymol. 324*, 342−55.
66. Pavel, E. G., Zhou, J., Busby, R. W., Gunsior, M., Townsend, C. A., and Solomon, E. I. (1998) *J. Am. Chem. Soc. 120*, 743−753.

BI026499M